Numerical Simulation of Particulate Fracture in Round Silicon Nitride Particulate/AA6061 Alloy Metal Matrix Composites

[1]B. Kotiveera Chari and A. Chennakesava Reddy[2]

[1]Professor, Department of Mechanical Engineering, NIT, Warnagal, Andhra Pradesh, India
[2]Assistant Professor, Department of Mechanical Engineering, MJ College of Engineering and Technology, Hyderabad, India
dr_acreddy@yahoo.com

Abstract: *Diagonal array unit cell/round particulate RVE models are used to predict particulate fracture using two-dimensional finite element methods under plane strain conditions. The particulate metal matrix composites are silicon nitride/AA6061 alloy at different volume fractions of silicon nitride. There is strong probability of silicon nitride particulate fracture at its high (30%) volume fraction in the AA6061 alloy matrix.*

Keywords: AA6061*, silicon nitride, round particle, RVE model, finite element analysis, particulate fracture.*

1. INTRODUCTION

Reinforcement materials for metal matrix composites can be produced in the form of continuous fibers, short fibers, whiskers, or particles. The parameter which is used to distinguish between these different forms of reinforcements is called the aspect ratio. The enhancement of specific stiffness, specific strength, wear and creep resistance, and the reduction of density and thermal expansion are a few of the most attractive features of particulate metal matrix composites-[1-4]. Davidson [5] has conducted the tensile and fracture toughness tests on 2011 Al alloy/silicon carbide (SiC) composite consisting of 15 vol. % SiC particulates. Overall tensile elongations values ranged from 1.6 to 2.4% and fracture toughness values from 18.7 to 29.5 MPa. Arsenault et al. [6] have studied the 0.5µm 20 vol. %, SiC spherical particles reinforced Al-1100, and they have observed that as the proof stress increases with increase in reinforcement content. Hertzberg [7] has reported that the particle size and shape are important factors in determining materials properties. Fatigue strength is greatly improved with the use of fine particles, and the uniform distribution of reinforcement is improved by matching the size of the reinforcement to the size of the matrix particles. Also, various particulates have been tested for micromechanical behavior. The particulate reinforcement materials other than silicon carbide and alumina are boron carbide [8-10], titanium boride [11-16] and silicon nitride [17-20].

The objective of this paper is to predict the particle fracture of silicon nitride/AA6061 alloy particulate metal matrix composites. Numerical simulation (finite element method) is employed to construct and analyze representative volume elements (RVEs) models of periodic circular particulates in a diagonal array distribution.

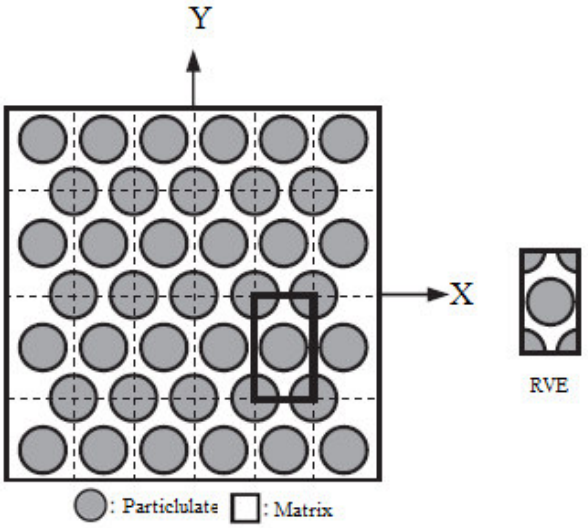

Figure 1: The RVE model: (a) particle distribution and (b) RVE scheme.

2. MATERIALS AND METHODS

The volume fractions of silicon nitride particle reinforcement were 10%, 20%, and 30% in the matrix AA6061 alloy. The periodic model for the representative volume element (RVE) scheme is shown in figure 1. The perfect adhesion was assumed between titanium boride particle and AA6061 alloy matrix. PLANE183 element was used for the matrix and the nanoparticle. The interface between particle and matrix was modeled using CONTACT -172 element. Also, an impact stressing simulations were performed for central (normal) impacts with finite element methods. Finite element analyses were performed at a velocity of 50 m/s.

If the particle deforms in an elastic manner (according to Hooke's law) then,

$$\tau = \frac{n}{2}\sigma_p \quad (1)$$

where σ_p is the particle stress and the n parameter used in this paper is given below:

$$n^2 = \frac{2}{E_p E_m}\left[\frac{E_p V_p + E_m V_m}{V_m/(4G_p)+1/(2G_m)\left((1/V_m)\ln(1/V_p)-1-(V_m/2)\right)}\right] \quad (2)$$

where E_p and G_P ate the particle elastic and shear moduli, E_m and G_m are the elastic and shear moduli of the matrix. V_p is the particle volume fraction and V_m is the volume fraction of matrix. If particle fracture occurs when the stress in the particle reaches its ultimate tensile strength, $\sigma_{p,uts}$, then setting the boundary condition at

$$\sigma_p = \sigma_{p,\,uts} \quad (3)$$

and substituting into Eq.(1) gives a relationship between the strength of the particle and the interfacial shear stress such that if

$$\sigma_{P,uts} < \frac{2\tau}{n} \quad (4)$$

Then the particle will fracture. Similarly if interfacial debonding/yielding is considered to occur when the interfacial shear stress reaches its shear strength

$$\tau = \tau_{max} \quad (5)$$

Then by substituting Eq. (5) into Eq.(1) a boundary condition for particle/matrix interfacial fracture can be established whereby,

$$\tau_{max} < \frac{n\sigma_p}{2} \quad (6)$$

This approach suggests that the outcome of a matrix crack impinging on an embedded particle depends on the balance between the particle strength and the shear strength of the interface.

3. RESULTS AND DISCUSSION

Influence of volume fraction on the elastic moduli, E_x, E_y and Gxy are shown figure 2a. The tensile elastic modulus increases with increase of volume fraction of silicon nitride. The compressive elastic modulus is nearly constant at three volume fractions of silicon nitride. The rigidity modulus decreases with increase of volume fraction of silicon nitride. The major Poisson's ratio is increases with increase of volume fraction of silicon nitride (figure 2b).

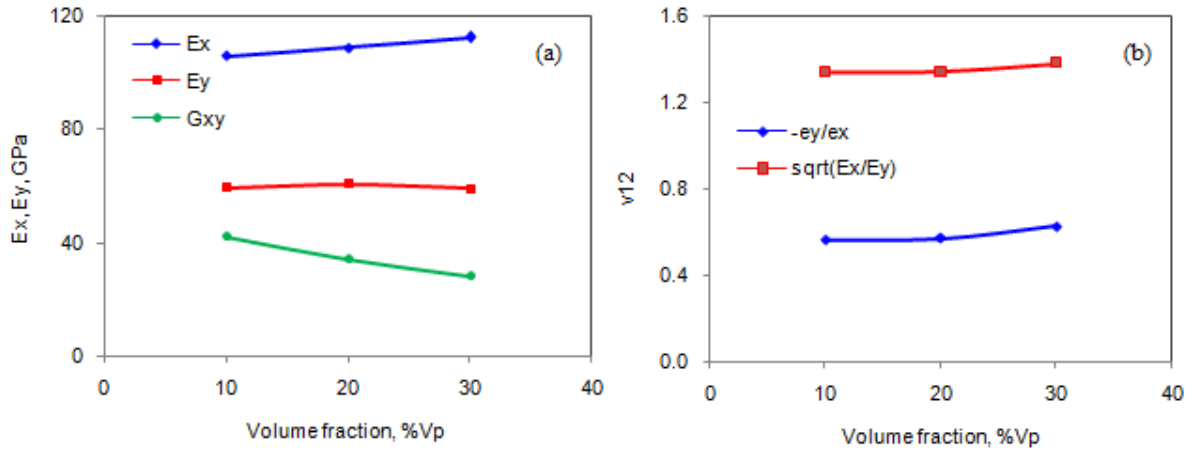

Figure 2: Effect of volume fraction on effective material properties.

The interfacial normal traction, t_n is about same for three volume fractions of silicon nitride as shown in figure 3. The trend of tangential traction, t_t is also same as that of normal traction with a phase difference and lesser amplitude. The interfacial normal

and tangential displacements are shown in figure 4. The normal and tangential displacements are higher for the low volume fraction of silicon nitride than those for the high volume fraction of silicon nitride. This is due to the decrease of ductility of the composite with increase of silicon nitride content in the composite.

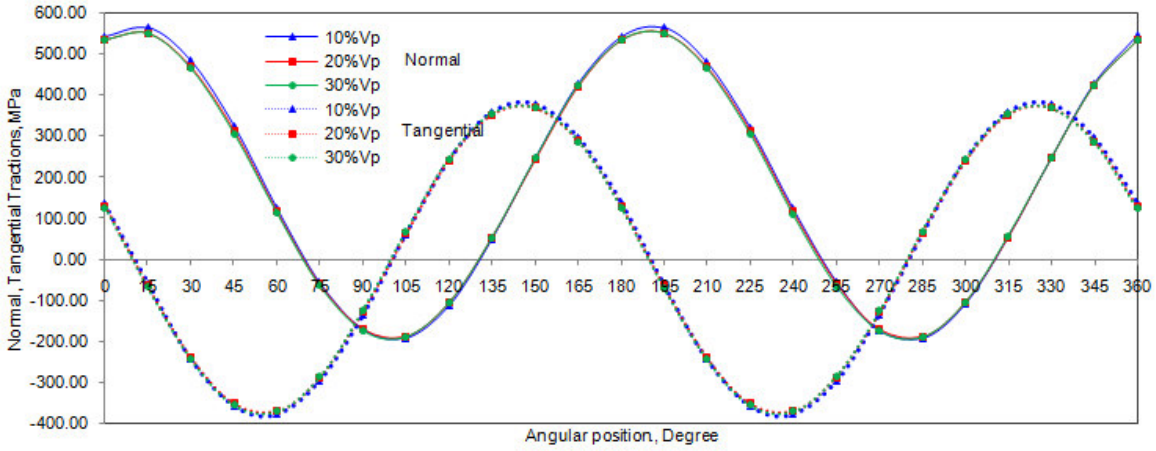

Figure 3: Interfacial tractions due to tensile loading.

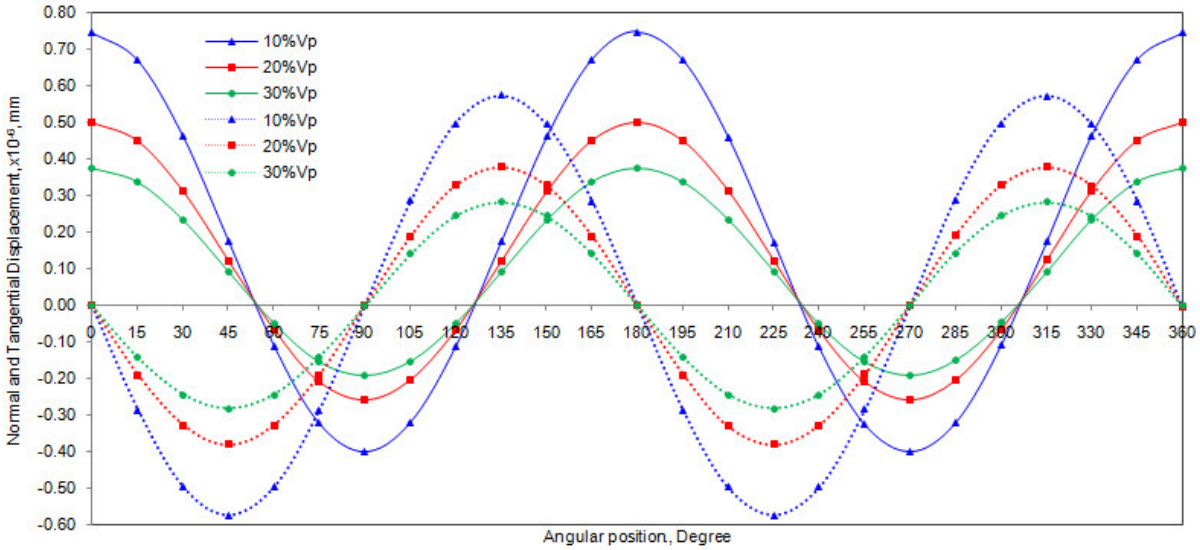

Figure 4: Interfacial displacements due to tensile loading.

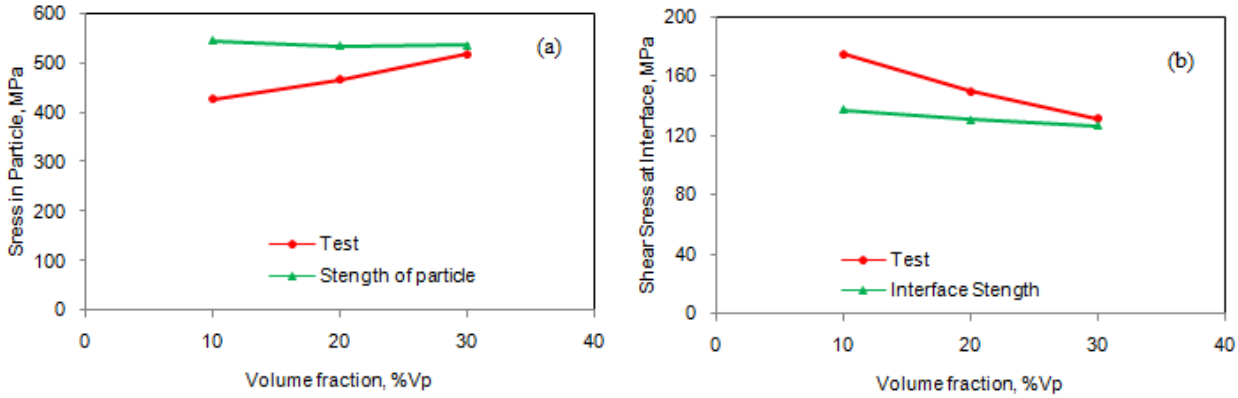

Figure 5: Fracture criteria of: (a) particulate and (b) interface.

The silicon nitride particulate fracture is occurred at 30% silicon nitride in the composite as per the condition $\sigma_p < 2\tau/n$ as shown in figure 5a. The condition for the occurrence of debonding is satisfied as shown in figure 5b. For silicon nitride less than 20% of volume fraction in the composite, the debonding is more prevailed. But at 30 % of silicon nitride in the composite, the particle strength is approximately equal to the interfacial shear stress. Figure 7 depicts the raster images of results obtained from the finite element analysis. The stress induced in the particle is lower than that induced at the interface between silicon nitride particulate and AA6061 alloy matrix (figure 6a) at 10% volume fraction, whereas it is higher in the particle that at the interface for 20% and 30% volume fractions. The shear stress developed at the interface is much higher than that induced in the silicon carbide particulate (figure 6b). Hence, there is a possibility of debonding at the interface between the particulate and the matrix at low volume fraction (10%) of silicon nitride and particulate fracture at high volume fraction (30%) of silicon nitride.

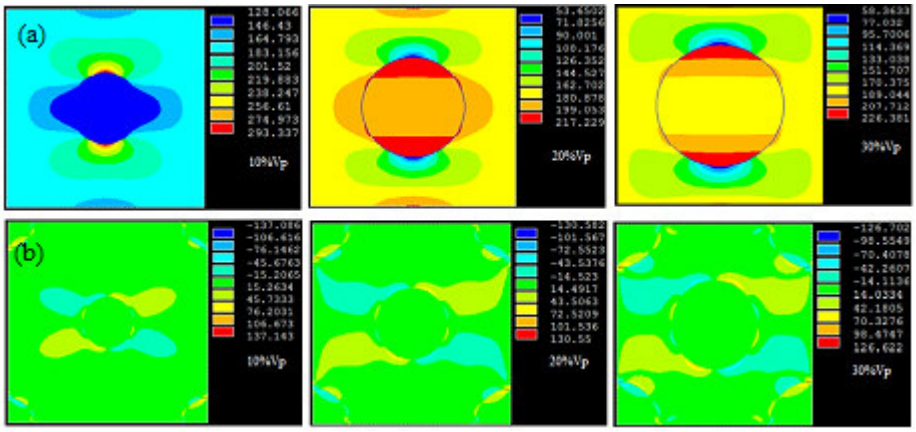

Figure 6: Results obtained from finite element analysis: (a) tensile stress and (b) shear stress.

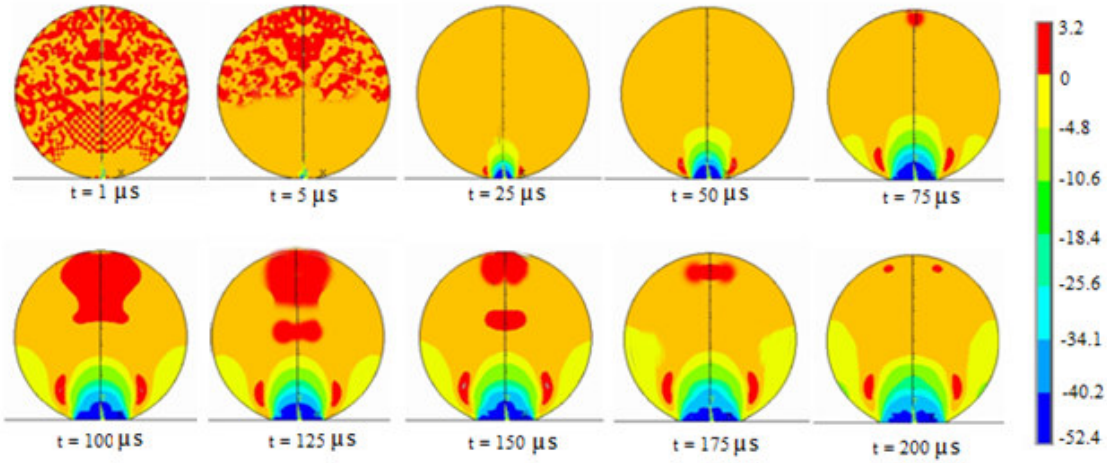

Figure 7: Impact analysis for silicon nitride particulate fracture (30% Vp of silicon nitride).

The stressing events and propagation of the stress waves with respect to time are shown in figure 8. It is seen that when the silicon nitride particulate is impacted, compressive and tensile stresses are generated inside the specimen. With the increase of impact time the area of contact deformation increases. Tensile waves are propagating from the impact side towards the low stressed side, i.e., towards the top side. At the boundary of the contact deformation, tensile stresses are generated and propagated, and in other parts compressive stresses are generated. The tensile stresses are generated around the contact deformation. Hence, the particulate fracture is the resultant effect of tensile and compression at mutual directions.

4. CONCLUSION

The silicon nitride particulate fractures at its high volume fraction (30%) in the composite. The debonding at the interface between silicon nitride at the AA6061 alloy matrix is predominant at low volume fractions. The particulate fracture is the resultant effect of tensile and compression at mutual directions for diamond array periodic distribution of round particles in AA6061 alloy matrix.

REFERENCES

1. R.J. Arsenault, Relationship between strengthening mechanisms and fracture toughness of discontinuous SiC/Al composites, Journal of Composites Technology, vol.10, 1988, pp.140-145.
2. D. L. McDaneals, Analysis of Stress, Strain, Fracture and Ductility Behavior of Al Matrix Composite Containing Discontinuous SiC Reinforcement, Metallurgical Transactions A, vol. 16A, 1985, pp. 1105-1115.
3. D. J. Lloyd, Particle Reinforced Al and Mg Matrix Composites, International Materials Reviews, vol. 39, No.1, 1994, pp. 1-23.
4. S.V. Kamat, J.P. Hirth, and R. Mehrabian, Mechanical properties of particulate-reinforced aluminum-matrix composites, Acta Metallurgica, vol.37, No.9, 1989, pp. 2395-2402
5. D. L. Davidson, Tensile Deformation and Fracture Toughness of 2014+15 vol pct SiC Particulate Composite, Metallurgical Transactions A, vol.22A, January 1991, pp. 113-123.
6. R. J. Arsenault, L.Wang, and C. R. Feng, Strengthening of composites due to microstructural changes in the matrix, Acta Metallurgia, vol.39, 1991, pp. 47-57.
7. R.W. Hertzberg, Deformation and Fracture Mechanics of Engineering Materials, 3rd ed., John Wiley & Sons, 1989.
8. S. Sundara Rajan and A. Chennakesava Reddy, Assessment of Tensile Behavior of Boron Carbide/AA2024 Alloy Metal Matrix Composites, 1st International Conference on Composite Materials and Characterization, Bangalore, March 1997, pp.160-163.
9. P. Martin Jebaraj and A. Chennakesava Reddy, Prediction of Micro-stresses and interfacial Tractions in Boron Carbide/AA6061 Alloy Metal Matrix Composites, 1st International Conference on Composite Materials and Characterization, Bangalore, March 1997, pp. 183-185.
10. B. Kotiveera Chari and A. Chennakesava Reddy, Computation of Micro-stresses and interfacial Tractions in Boron Carbide/AA7020 Alloy Metal Matrix Composites, 1st International Conference on Composite Materials and Characterization, Bangalore, March 1997, pp. 186-188.
11. A. Chennakesava Reddy, Reckoning of Micro-stresses and interfacial Tractions in Titanium Boride/AA2024 Alloy Metal Matrix Composites, 1st International Conference on Composite Materials and Characterization, Bangalore, March 1997, pp. 195-197.
12. H. B. Niranjan and A. Chennakesava Reddy, Determination of Micro-stresses and interfacial Tractions in Titanium Boride/AA1100 Alloy Metal Matrix Composites, 1st International Conference on Composite Materials and Characterization, Bangalore, March 1997, pp. 192-194.
13. A. Chennakesava Reddy, Interfacial Debonding Analysis in Terms of Interfacial Tractions for Titanium Boride/AA3003 Alloy Metal Matrix Composites, 1st National Conference on Modern Materials and Manufacturing , Pune, 19-20 December, 1997.
14. P. Martin Jebaraj, A. Chennakesava Reddy, Effect of Interfacial Debonding on Stiffness of Titanium Boride/AA5050 Alloy Metal Matrix Composites, 1st National Conference on Modern Materials and Manufacturing , Pune, 19-20 December, 1997.
15. S. Sundara Rajan, A. Chennakesava Reddy, Micromechanical modeling of Titanium Boride/AA7020 Alloy Metal Matrix Composites in Finite Element Analysis using RVE Model, 1st National Conference on Modern Materials and Manufacturing, Pune, 19-20 December, 1997.
16. P. Martin Jebaraj, A. Chennakesava Reddy, Effect of Interfacial Tractions of Rectangular Titanium Boride Particulate/AA8090 Alloy Metal Matrix Composites , 1st National Conference on Modern Materials and Manufacturing, Pune, 19-20 December, 1997.
17. S. Sundara Rajan, A. Chennakesava Reddy, Cohesive Zone interfacial debonding of Silicon Nitride/AA1100 Alloy Metal Matrix Composites Using Finite Element Analysis , 1st National Conference on Modern Materials and Manufacturing, Pune, 19-20 December, 1997.
18. S. Sundara Rajan, A. Chennakesava Reddy, Simulation of Micromechanics for interfacial debonding in Silicon Nitride/AA2024 Alloy Metal Matrix Composites , 1st National Conference on Modern Materials and Manufacturing, Pune, 19-20 December, 1997.
19. P. Martin Jebaraj, A. Chennakesava Reddy, Finite Element Analysis for Assessment of Dislocation and Debonding Events in Silicon Nitride/AA3003 Alloy Metal Matrix Composites, 1st National Conference on Modern Materials and Manufacturing, Pune, 19-20 December, 1997.
20. A. Chennakesava Reddy, Evaluation of Debonding and Dislocation Occurrences in Rhombus Silicon Nitride Particulate/AA4015 Alloy Metal Matrix Composites, 1st National Conference on Modern Materials and Manufacturing, Pune, India, 19-20 December, 278-282, 1997.